Strain-Induced Stereoselective Formation of Blue-Emitting Cyclostilbenes

ARTICLE *in* JOURNAL OF THE AMERICAN CHEMICAL SOCIETY · SEPTEMBER 2015

Impact Factor: 12.11 · DOI: 10.1021/jacs.5b06258

9 AUTHORS, INCLUDING:

Minh Tuan Trinh

Columbia University

34 PUBLICATIONS **732** CITATIONS

SEE PROFILE

Michael Steigerwald

Columbia University

216 PUBLICATIONS **11,642** CITATIONS

SEE PROFILE

JACS
JOURNAL OF THE AMERICAN CHEMICAL SOCIETY

Article

pubs.acs.org/JACS

Strain-Induced Stereoselective Formation of Blue-Emitting Cyclostilbenes

Qishui Chen, M. Tuan Trinh, Daniel W. Paley, Molleigh B. Preefer, Haiming Zhu, Brandon S. Fowler, X.-Y. Zhu,* Michael L. Steigerwald,* and Colin Nuckolls*

Department of Chemistry, Columbia University, New York, New York 10027, United States

Supporting Information

ABSTRACT: We describe the synthesis of two conjugated macrocycles that are formed from the end-to-end linking of stilbenes. We have named these macrocycles cyclostilbenes. The two cyclostilbene isomers created in this study differ in the configuration of the double bond in their subunits. These macrocycles are formed selectively through a stepwise reductive elimination from a tetraplatinum precursor and subsequent photoisomerization. Single-crystal X-ray diffraction reveals the formation of channel architectures in the solid state that can be filled with guest molecules. The cyclostilbene macrocycles emit blue light with fluorescence quantum yields that are high (>50%) and have photoluminescence lifetimes of ∼0.8−1.5 ns. The breadth and large Stokes shift in fluorescence emission, along with broad excited-state absorption, result from strong electronic−vibronic coupling in the strained structures of the cyclostilbenes.

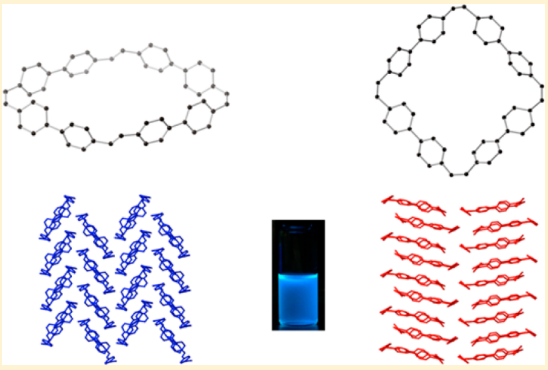

INTRODUCTION

Here we describe a new conjugated belt, formed by linking stilbene subunits into macrocycles, i.e., a cyclostilbene. The molecules in this study are members of a growing class of conjugated macrocycles,[1,2] such as cyclo-*para*-phenylenes (CPPs),[3−5] cyclothiophenes (CTs),[6−8] and cycloporphyrins (CPs).[9−11] The advent of synthetic methods to form strained conjugated macrocycles over the past few years is enabling the formation of new cyclic structures that heretofore were difficult to make. The three main approaches to making strained conjugated macrocycles are (1) using statistical oligomerization of precursors with curvature,[7,12,13] (2) synthesizing an unstrained cyclic precursor followed by an efficient reaction that introduces strain,[4,14,15] or (3) using a template to aid in the formation of the macrocycle.[9,16] A wealth of new materials can result from these new types of cyclic conjugated oligomers that have well-defined sizes and shapes. For example, conjugated macrocycles are useful as supramolecular nanostructures, such as columnar tubes or inclusion complexes.[17−20] The design strategy to yield interesting structural, optical, and electronic properties for cyclic conjugated macrocycles is different than that for linear conjugated molecules.[21] Within this context, we investigated the formation of cyclostilbenes by the end-to-end linking of stilbenes into macrocycles. We show in Figure 1 three stereoisomers, **1-CTCT**, **2-CCCC**, and **3-TTTT**, that differ in the number of *trans* (T) and *cis* (C) double bonds in the stilbene subunits.

Stilbene is a prototypical subunit used in many conjugated oligomers and polymers, such as poly(phenylenevinylene),[22] yet it has not been studied extensively in cyclic structures. The optical and electronic properties of stilbene are extremely sensitive to both the environment and the conformation of the stilbene.[23,24] Large cyclophanes linked with unsaturated bridges have been extensively studied for their electrochemical properties, and strong diamagnetic ring currents were observed in their dianions.[25,26] However, their low-yielding and nonselective syntheses[27−29] precluded their being studied fully. In this article, we describe a new selective synthesis of two cyclostilbenes, **1-CTCT** and **2-CCCC**. **1-CTCT** has alternating *cis* and *trans* double bonds and forms stereoselectively from the four-fold reductive elimination of a tetranuclear square-planar platinum macrocycle. **2-CCCC** can be formed quantitatively by UV irradiation of **1-CTCT**. Our approach gives precise control over the final product structures. We find that these molecules are strong blue-emitting materials that can act as supramolecular hosts and pack in tubular structures in the solid state.

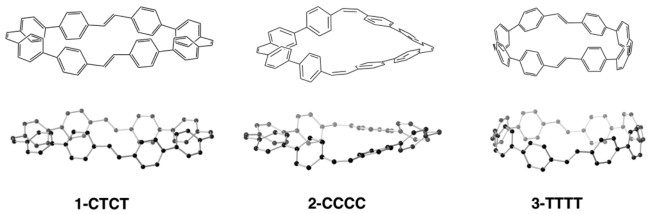

Figure 1. Structures of cyclostilbenes **1-CTCT**, **2-CCCC**, and **3-TTTT** calculated at the B3LYP/6-31G** level.

Received: June 23, 2015
Published: September 16, 2015

DOI: 10.1021/jacs.5b06258
J. Am. Chem. Soc. 2015, 137, 12282−12288

RESULTS AND DISCUSSION

Synthesis. Scheme 1 shows the method developed to synthesize cyclostilbene **1-CTCT**. We based our strategy on those of Yamago and co-workers for the synthesis of CPPs[4] and Bäuerle and co-workers for the synthesis of CTs.[30] Here, we utilize (*E*)-4,4′-bis(trimethylstannyl)stilbene in combination with $Pt(COD)Cl_2$ (COD = 1,5-cyclooctadiene) to form the square tetranuclear platinum complex **5** in 84% yield. Figure S13 shows the crystal structure of **5**, confirming that all four stilbene units retain the *trans* geometry of the olefin. Reductive elimination (upon addition of 10 mol equiv of PPh_3) forms the cyclostilbene in 28% yield. The direct 4-fold reductive elimination would yield cyclostilbene **3-TTTT**; however, the macrocycle that we isolate is **1-CTCT**, in which two of the double bonds have isomerized to the *cis*-olefin. The reaction is stereoselective, in that we do not isolate or detect any of the other stereoisomers with a different arrangement of *cis* and *trans* double bonds. Under UV irradiation, **1-CTCT** quantitatively converts to isomer **2-CCCC**. This isomer had been previously synthesized in a poor yield (~1%) via a four-fold Wittig reaction.[31]

Scheme 1. Synthesis of Macrocycle 1-CTCT[a]

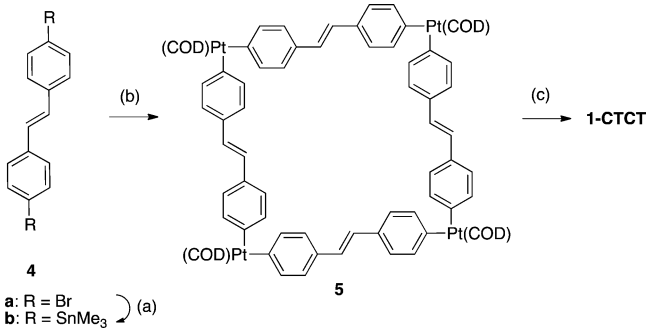

[a]Reagents and conditions: (a) *i.* *n*-BuLi, THF, −78 °C, 3 h; *ii.* $SnMe_3Cl$, −78 °C to rt, 12 h, 78%. (b) $Pt(COD)Cl_2$, 1,2-dichloroethane, 75 °C, 20 h, 84%. (c) PPh_3, toluene, 100 °C, 24 h, 28%.

We isolate both **1-CTCT** and **2-CCCC** as light yellow solids. Unlike their unsubstituted linear counterparts,[32,33] cyclostilbenes are soluble in common organic solvents such as dichloromethane (DCM), tetrahydrofuran (THF), and chloroform ($CHCl_3$). They are insoluble in toluene and methanol (MeOH). Both isomers are air-stable and can be kept in the ambient for extended periods of time without change. Neither stereoisomer (**1-CTCT** or **2-CCCC**) shows any mass loss up to 400 °C (for the thermogravimetric analysis data, see the Supporting Information, Figures S8 and S9). The two isomers behave similarly upon electrochemical reduction. We measured their reduction potentials using cyclic voltammetry (CV) in THF solution with Bu_4NPF_6 (0.1 M) as the electrolyte. The cyclostilbenes show reversible reduction events, with a reduction onset potential of −1.26 V for **1-CTCT** and −1.28 V for **2-CCCC** versus the ferrocene/ferrocenium (Fc/Fc^+) redox couple (see Supporting Information, Figure S18). The calculated lowest unoccupied molecular orbital (LUMO) levels are essentially the same for **1-CTCT** and **2-CCCC**.

Crystal Structures. We were able to grow single crystals suitable for X-ray diffraction for both isomers. After extensively screening solvent combinations, we found that **1-CTCT** forms crystals by layering of toluene on a THF solution of the macrocycle and that **2-CCCC** forms crystals by layering of MeOH on a DCM solution of the macrocycle. Figure 2a shows the top view of cyclostilbene **1-CTCT**. The macrocycle crystallizes as a 1:1 inclusion complex, **1-CTCT**·toluene. The molecule adopts an ellipsoidal shape, with the long axis (19.1 Å) nearly twice the length of the short axis (9.7 Å). The two stacked *trans*-stilbene moieties deviate away from planarity by ~19° [C—C═C—C dihedral angle = 161.0(11)°]. The angles at the sp^2 carbons of the *cis* and *trans* double bonds are slightly expanded to between 121.8(11)° and 128.3(10)°. The biphenyl units have a wide range of Ar—Ar twist angles between

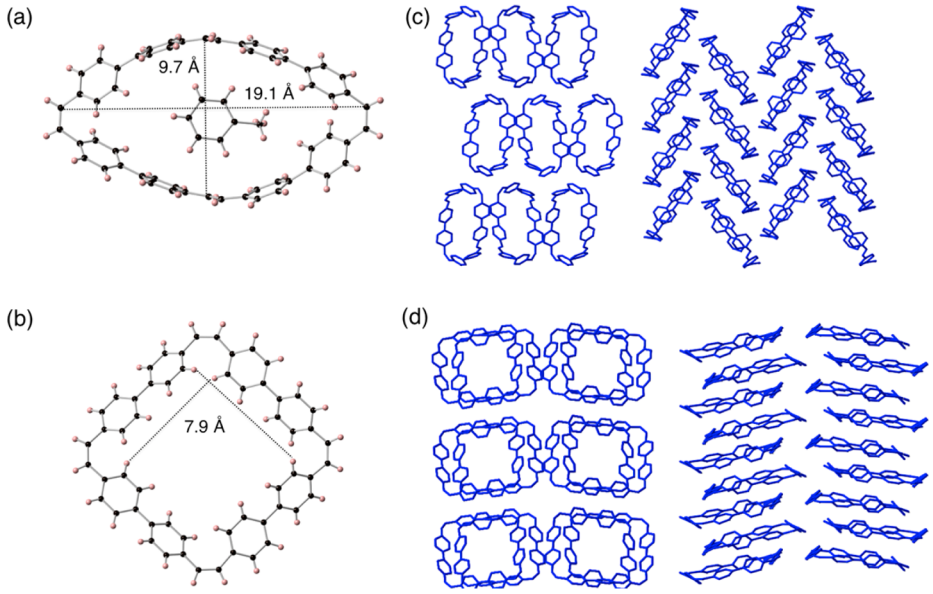

Figure 2. Single-crystal X-ray diffraction structure of (a) **1-CTCT**·toluene and (b) **2-CCCC** from top view. Disordered DCM solvent molecules are removed for clarity. Packing structure of (c) **1-CTCT** along the (100) and (302) planes and (d) **2-CCCC** along the (001) and (102) planes. Hydrogen atoms and solvent molecules are removed.

DOI: 10.1021/jacs.5b06258
J. Am. Chem. Soc. 2015, 137, 12282−12288

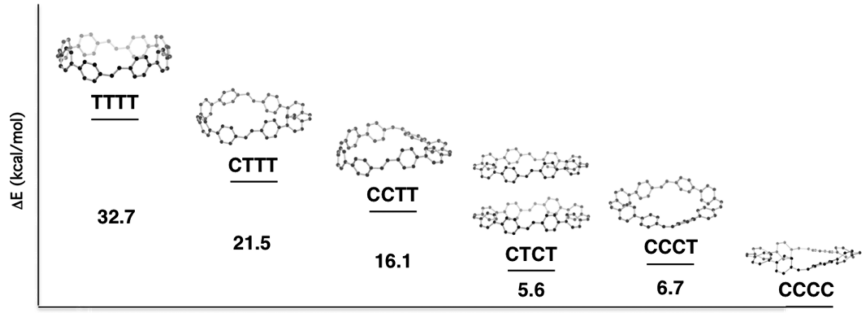

Figure 3. Structures and relative energies of cyclostilbene isomers calculated at the B3LYP/6-31G** level. Energy values are in kcal/mol, and compared with the lowest energy isomer **2-CCCC**.

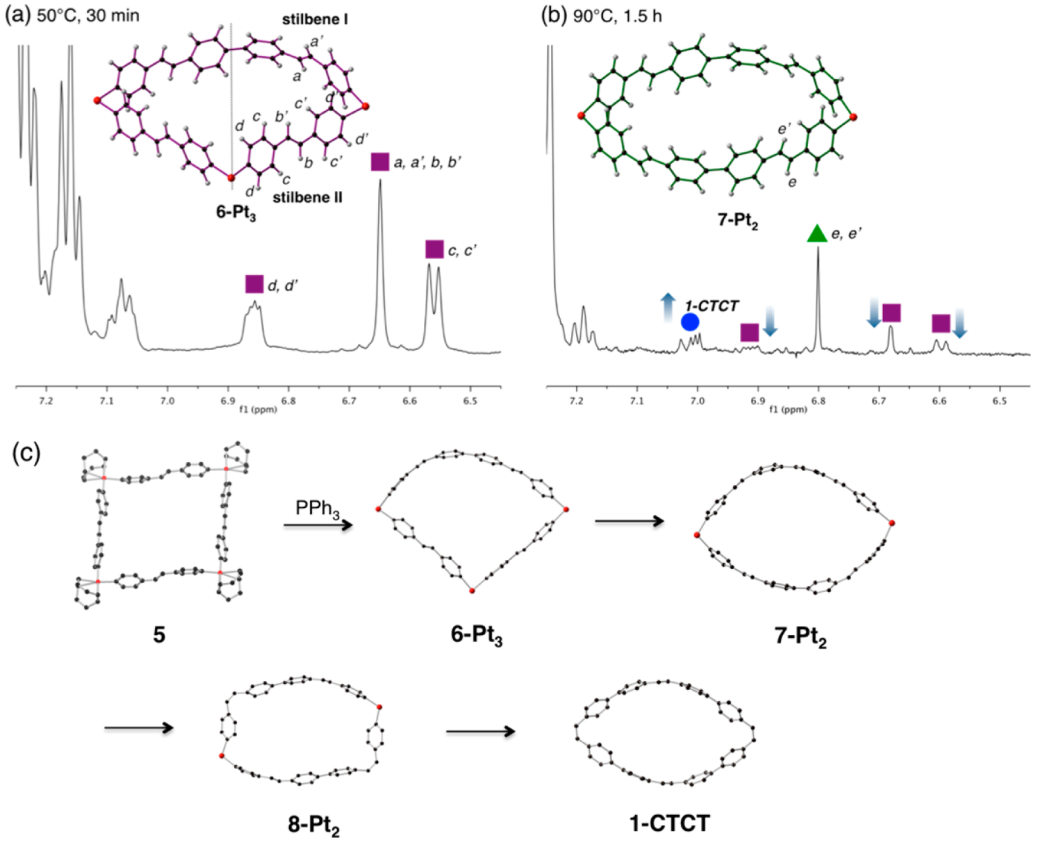

Figure 4. Aromatic region of the ^{1}H NMR spectra of two reaction intermediates (a) **6-Pt$_3$** and (b) **7-Pt$_2$**. (c) Proposed mechanism of stepwise reductive elimination to stereoselectively form isomer **1-CTCT**. Hydrogen atoms in (c) and phosphine ligands in all structures are removed for clarity. Red, platinum; black, carbon; gray, hydrogen.

21.3(17)° and 51.5(15)°. The packing of **1-CTCT** in the solid state is similar to that of [8]-, [9]-, [10]-, and [12]-CPP.[19] The molecules stack in tubular structures along the *a*-axis direction, and the tubes pack in a herringbone pattern (Figure 2c).

Isomer **2-CCCC** has a different shape and a smaller inner cavity than **1-CTCT**. As shown in Figure 2b, the macrocycle is square-shaped. The cavity measures 7.9 Å from the edge of one phenyl to the edge of the other phenyl across the macrocycle (Figure 2b). The cavity is filled with disordered DCM molecules from the crystallization. The angles at the sp^2 carbons of the *cis* double bonds are more expanded than **1-CTCT** to between 129.5(2)° and 133.1(2)°. The biphenyl units are nearly coplanar, and the Ar−Ar dihedral angles range from 9.2(3)° to 26.3(3)°. Similar to **1-CTCT**, channel architectures form in the packing of **2-CCCC**, as the molecules stack with their cavities over each other along the *c*-axis direction. The channels are smaller in **2-CCCC** than in **1-CTCT** because for **2-CCCC** the molecules slip stack with respect to their neighbors. This slip stacking can be seen in the alternating layers in Figure 2d. The channels in **2-CCCC** are also more continuous than in **1-CTCT**, which caused several challenges in the crystal structure determination. DCM easily diffuses out of the channels, which causes the crystals to shatter rapidly when in contact with oil. The continuous solvent-filled channels also cause extensive crystallographic disorder.

The π-systems around the peripheries are oriented differently in **1-CTCT** and **2-CCCC**. The p-orbitals are aligned essentially perpendicular to the plane of the macrocycle in **2-CCCC**, whereas they are aligned radially in **1-CTCT** (excepting those of its two *cis* C═C bonds). This orientation difference is

DOI: 10.1021/jacs.5b06258
J. Am. Chem. Soc. 2015, 137, 12282−12288

controlled by varying the geometry of the double bond in the macrocycle and plays an important role in both the strain energies and the excited-state properties of the molecule, as discussed in the following sections.

Stereoselective Isomerization. Although examples of conjugated macrocyclic isomers containing *cis* (C) or *trans* (T) olefins are known, the stereochemistry is built in during their synthesis, using typically Wittig or McMurry reactions.[26,34−36] Our observation of isomerization from a TTTT precursor to give stereoselectively a CTCT isomer is unusual. We used density functional theory (DFT) calculations to gain insight into the different cyclostilbene isomers. Figure 3 shows the optimized geometries and relative energies of all six possible cyclostilbene isomers. The CCCC geometry is the lowest in energy, and we use its total energy as the zero benchmark. The next most stable configuration is CTCT, which is 5.6 kcal/mol higher in energy, followed by CCCT. The least stable isomer, TTTT, is 32.7 kcal/mol higher in energy than the all *cis* macrocycle. We note that for **1-CTCT**, there exists two conformers: one where the two *trans*-stilbene units mirror each other (bottom structure in Figure 3), and one where they exhibit C_2 symmetry (top structure in Figure 3). DFT calculations indicate that they are isoenergetic (see Supporting Information).

We estimated the ring strain energies for **1-CTCT** and **2-CCCC** using isodesmic comparisons,[37] and found values of 17.0 kcal/mol for the former and 0.1 kcal/mol for the latter (see Supporting Information). The large contrast between the differences in energies of the macrocycles (5.6 kcal/mol) and their strain energies (16.9 kcal/mol) highlights the greater ability of the *cis* olefin to support the ring shape. For a stilbene monomer, the *cis* isomer is more sterically hindered and higher in energy than *trans*, whereas in the macrocycle the *trans*-stilbene subunit needs to bend its π-system to accommodate the curvature of the belt structure. Therefore, the larger strain in **1-CTCT** accounts for the 5.6 kcal/mol difference mentioned above, as well as the intrinsically higher energy of the *cis*-stilbene subunit in the acyclic isodesmic partners.

Uncatalyzed, thermal *trans*-to-*cis* isomerization is known for overcrowded ethylene systems, where steric effects lower the activation barriers due to destabilization of strained ground-state conformations.[38] Similarly, it is possible that the highly strained **3-TTTT** isomer is initially formed from direct reductive elimination of Pt macrocycle **5**, and then isomerizes to a more stable isomer **1-CTCT** to reach an energy minimum. However, this cannot explain the fact that **1-CTCT** is formed exclusively in the reaction and not a thermodynamically controlled ratio of different products. Therefore, instead of a direct 4-fold reductive elimination to yield **3-TTTT**, it is more likely that the stereoselective isomerization occurs during the multi-step reductive elimination process.

In order to follow the cascade of reactions that lead from **5** to the ultimate product **1-CTCT** and further understand the stereoselective isomerization process, we monitored the reaction in $C_2D_2Cl_4$ by ^{1}H NMR. Figure 4 shows the downfield region (δ = 6.5−7.0 ppm) of the ^{1}H NMR spectrum that is remote from the aryl phosphine resonances. Within this region, we are able to observe the partial spectra of two intermediates during the reaction. Upon addition of PPh_3 and heating to 50 °C, three resonances emerge that have equal integrated intensities, suggesting that it is not simply the ligand-exchange product containing four platinum centers, in which the resonances would integrate 2:2:1.

We assign this new species to the fan-shaped intermediate **6-Pt$_3$**, in which one platinum center has been eliminated. In this structure, there are two types of stilbene units present—*stilbene I* and *stilbene II*—and there are two of each type. The two *stilbene I* units are those that had been bonded to the now-eliminated Pt center, and they are now bonded to one another to give the arced arm of **6-Pt$_3$**. Each of the two *stilbene II* units retains both of its Pt termini, forming a straight arm of **6-Pt$_3$**. The phenyl resonances in *stilbene II* are shifted upfield to the stilbene olefin region due to PPh_3-ligated Pt(II), whereas in *stilbene I* the phenyl protons are shifted downfield, outside the clean spectrum window. The seemingly simple spectral pattern can be deconvoluted by COSY and HSQC experiments (Figures S14 and S15), and Figure 4a displays the assignment of the resonances.

When we heat **6-Pt$_3$** to 90 °C, we observe the formation of a second intermediate, as well as the fully eliminated product **1-CTCT** (Figure 4b). This second intermediate has only one resonance in this window of the spectrum, suggesting the highly symmetrical structure **7-Pt$_2$**. The observed resonance corresponds to both olefin protons. Each of the phenyl protons is buried underneath the phosphine region as those of *stilbene II* in **6-Pt$_3$**. Consistent with reductive elimination from platinum biaryls being a first-order reaction,[39,40] both the decay of **6-Pt$_3$** and the formation of **1-CTCT** over time fit to a single exponential (Figures S16 and S17).

Therefore, by combining the NMR experimental observations and DFT calculations (see Supporting Information), we propose a stepwise platinum reductive elimination mechanism for the stereoselective formation of **1-CTCT** (Figure 4c). There is a great amount of curvature in the *trans*-stilbene units in **7-Pt$_2$**, and the formation of an additional aryl−aryl bond would introduce even more distortion, making reductive elimination unfavorable compared to other processes such as homolytic cleavage to give linear oligomers instead of the desired cyclic product.[30,41] The other pathway for **7-Pt$_2$** is thermal isomerization of the *trans* double bonds to the *cis* conformation. The stereochemical isomerization occurs because this isomerization pattern gives rectangular-shaped **8-Pt$_2$** that is the most favorable pathway to release strain from **7-Pt$_2$**. From this structure, reductive elimination proceeds rapidly to form cyclostilbene **1-CTCT**, and **8-Pt$_2$** is not observable on the NMR time scale.

Photophysics. Figure 5a displays the UV−vis absorption and fluorescence emission spectra for **1-CTCT** and **2-CCCC**. A striking feature is that both cyclostilbenes show broad blue emission and large Stokes shifts. Table 1 summarizes the photophysical data for **1-CTCT** and **2-CCCC**. The maximum absorption of cyclostilbene **1-CTCT** shifts slightly to the red from that of **2-CCCC**. Time-dependent DFT (TD-DFT) calculations indicate that the highest occupied molecular orbital (HOMO)→LUMO transition is symmetry forbidden in both molecules. This is similar to what is observed for CPPs and other symmetrical, conjugated macrocycles.[42] The absorption peak in the UV region arises from a π−π^* excitation that is a combination of HOMO−1→LUMO and HOMO→LUMO+1 transitions with a high oscillator strength (f). Our calculations indicate that this transition occurs from primarily the olefin (the *trans* olefin in the case of **1-CTCT**) to its π^* orbital (Figure S23). The lower-energy shoulder peak corresponds to the HOMO→LUMO transition (arrow in Figure 5a). This is due to dynamic conformational changes in solution that break symmetry and result in nonzero f values.

DOI: 10.1021/jacs.5b06258
J. Am. Chem. Soc. 2015, 137, 12282−12288

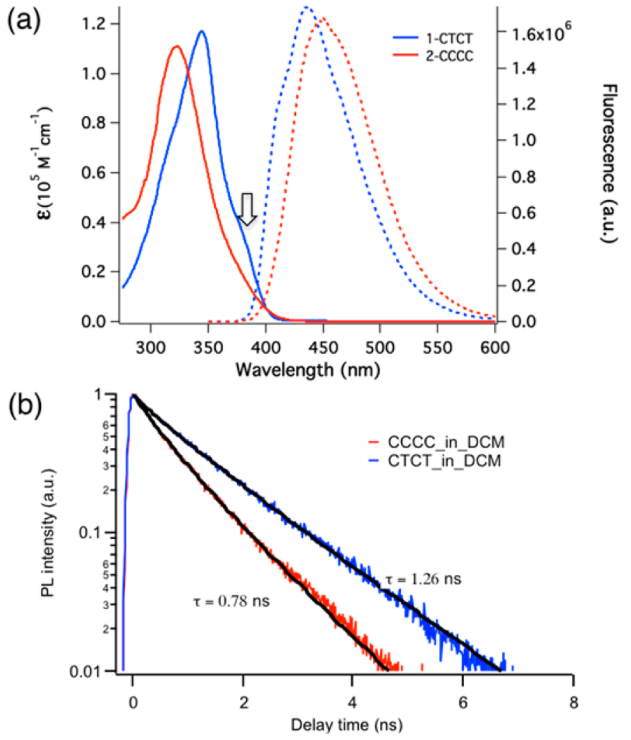

Figure 5. (a) UV−vis absorption spectra of **1-CTCT** (blue, solid line) and **2-CCCC** (red, solid line), 1×10^{-5} M in DCM. Fluorescence spectra of **1-CTCT** (blue, dashed line) excited at 340 nm and **2-CCCC** (red, dashed line) excited at 320 nm, 1×10^{-6} M in DCM. The arrow indicates the shoulder peak that corresponds to the HOMO→LUMO transition. (b) Normalized photoluminescence decay kinetics of **1-CTCT** (blue) and **2-CCCC** (red) in DCM solution and their fits (black).

Table 1. Photophysical Data for 1-CTCT and 2-CCCC

	absorption	emission			
	λ_{max}/nm	λ_{max}/nm	Φ_F[a]	τ_F/ns	k_r[b]/10^8 s^{-1}
1-CTCT	344	436	0.56	1.26	4.44
2-CCCC	322	450	0.55	0.78	7.18

[a]Coumarin 1 (Φ_F = 0.79 in air) was used as a reference for fluorescence quantum yield calculations (see Supporting Information). [b]Radiative decay rate constants from the excited singlet state, given by the equation $\Phi_F = k_r\tau_F$.

Both **1-CTCT** and **2-CCCC** show high photoluminescence quantum yields (PLQYs) above 50%, similar to [9]- and [10]-CPP.[42,43] The high PLQYs for the cyclostilbenes are surprising because the S_0−S_1 transition is dipole forbidden, with minimal or no oscillator strength in the S_1 state. Calculations[44] revealed that, in large CPP molecules, S_1 strongly couples with vibrational modes, resulting in a self-trapped localized excitonic state (S_1*) with a nonzero dipole transition that facilitates strong emission. Similarly, the emission from the cyclostilbenes also comes from S_1* state (Figure 6c) with high PLQYs. The absorption and emission processes taking place from different electronic states also explains the large Stokes shift for these cyclostilbenes. The structures of **1-CTCT** and **2-CCCC** in their excited states are highly strained. This strain results in a strong coupling of the excited states with the vibrational modes yielding the vibronic bands observed in the emission spectra. Figure S18 shows the emission spectra of **1-CTCT** that is fitted by three Gaussian functions with the peaks centered at 2.706, 2.886, and 3.049 eV. The differences in energy between these peaks are 0.18 and 0.163 eV, corresponding to the phenylene stretching vibration mode.[45]

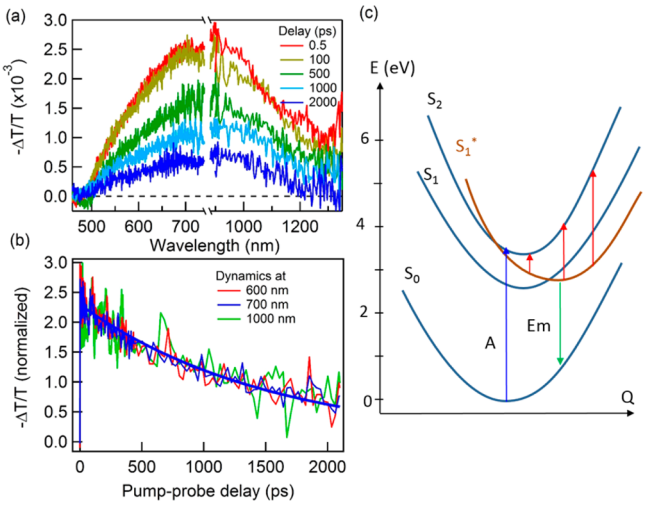

Figure 6. Transient absorption spectra at various pump−probe delays (a) and exciton dynamics at different probe wavelengths (b) for **1-CTCT** upon 325 nm excitation. (c) Schematic illustration of optical transition and relaxation in cyclostilbenes. The energy levels for S_1 and S_2 obtained from the calculations (see Supporting Information), but not for S_1*. A and Em represent absorption and emission, respectively. Red arrows depict the excited-state absorption. Q is the coordinate.

Time-resolved fluorescence decay kinetics for **1-CTCT** and **2-CCCC** dissolved in DCM are shown in Figure 5b. Their excited-state decay kinetics are similar to a slightly longer lifetime for **1-CTCT**. The values are of fluorescence quantum yield (Φ_F), fluorescence lifetime (τ_F), and radiative decay rates (k_r) for both cyclostilbenes are summarized in Table 1. The radiative decay rates for both macrocycles are similar, and this is not surprising given that k_r is closely related to the oscillator strength.[46] It is known that excited alkenes can undergo adiabatic isomerization.[47] To examine this, we encapsulated both molecules in polystyrene film and measured the time-resolved PL decay kinetics as a function of temperature (Figure S21). The PL decay kinetics of both molecules show very little dependence on temperature (down to 88 K), precluding the isomerization process for these macrocyles.

Transient Absorption Spectroscopy. To further study the role of electron−phonon coupling in these molecules, we performed transient absorption spectroscopy on **1-CTCT**. Figure 6 shows differential transmission ($-\Delta T/T$) spectra and exciton dynamics for **1-CTCT** in $CHCl_3$ upon 325 nm excitation. Interestingly, we observed a very broad excited-state absorption from the visible to near-IR range. The dynamics at different wavelengths are described by the same lifetime of 1500 ± 40 ps (Figure 6b), indicating that they originate from a single species. The large structural change suggested by fluorescence measurements can also explain the broad transient absorption feature, as illustrated in Figure 6c. The optically bright S_2 state from initial optical excitation can rapidly relax to the twisted S_1* state. The broad transient absorption from S_1* to S_2 can be attributed to the large offset in equilibrium nuclear coordinates, i.e., large reorganization energy, as illustrated by the red arrows.

DOI: 10.1021/jacs.5b06258
J. Am. Chem. Soc. 2015, 137, 12282−12288

CONCLUSION

In summary, we have revealed a method to stereoselectively synthesize two members of the cyclostilbene family of conjugated macrocycles. This unusual reaction sequence is programmed by the four-fold reductive elimination of Pt centers to produce the strained, conjugated macrocycle. **1-CTCT** has not previously been reported and would be difficult to make by traditional methods. This synthetic method now allows these two macrocycles to be studied that differ only in the configuration of the stilbene double bonds. We have shown here that it is possible to create materials that have different channel architectures in the solid state and different excited-state geometries. The cyclostilbenes are suitable hosts to form inclusion complexes, which augurs well for the creation of optoelectronic devices whose properties can be varied by changing the guest that is included. The molecules begin to fill the void in studies of the material properties of conjugated macrocycles. The macrocycles emit blue light with high quantum yields due to their rigid, cyclic configuration providing strong coupling between their excited states and vibrational modes. This study also leaves a challenge to find a method to create the all *trans*-cyclostilbene that has heretofore been unattainable.

ASSOCIATED CONTENT

Supporting Information

The Supporting Information is available free of charge on the ACS Publications website at DOI: 10.1021/jacs.5b06258.

Synthetic procedures, ^{1}H and ^{13}C NMR spectra, TGA analysis, NMR kinetic experiments, PLQY measurements, transient absorption measurements, and computational details (PDF)

X-ray crystallographic data for **2-CCCC** (CIF)

X-ray crystallographic data for **1-CTCT** (CIF)

X-ray crystallographic data for **5** (CIF)

AUTHOR INFORMATION

Corresponding Authors

*xz2324@columbia.edu

*mls2064@columbia.edu

*cn37@columbia.edu

Notes

The authors declare no competing financial interest.

ACKNOWLEDGMENTS

Primary support for this project was provided by the Chemical Sciences, Geosciences and Biosciences Division, Office of Basic Energy Sciences, U.S. Department of Energy (DOE), under award no. DE-FG02-01ER15264. X.-Y.Z. acknowledges support by the U.S. National Science Foundation grant DMR 1321405. Single-crystal X-ray diffraction analysis was performed at the Shared Materials Characterization Laboratory (SMCL) at Columbia University. Use of the SMCL was made possible by funding from Columbia University. Research was carried out in part at the Center for Functional Nanomaterials, Brookhaven National Laboratory, which is supported by the U.S. DOE, Office of Basic Energy Sciences, under contract no. DE-AC02-98CH10886.

REFERENCES

(1) Iyoda, M.; Yamakawa, J.; Rahman, M. J. *Angew. Chem., Int. Ed.* **2011**, *50*, 10522−10553.

(2) Kawase, T.; Kurata, H. *Chem. Rev.* **2006**, *106*, 5250−5273.

(3) Golder, M. R.; Jasti, R. *Acc. Chem. Res.* **2015**, *48*, 557−566.

(4) Yamago, S.; Watanabe, Y.; Iwamoto, T. *Angew. Chem., Int. Ed.* **2010**, *49*, 757−759.

(5) Segawa, Y.; Miyamoto, S.; Omachi, H.; Matsuura, S.; Senel, P.; Sasamori, T.; Tokitoh, N.; Itami, K. *Angew. Chem., Int. Ed.* **2011**, *50*, 3244−3248.

(6) Krömer, J.; Rios-Carreras, I.; Fuhrmann, G.; Musch, C.; Wunderlin, M.; Debaerdemaeker, T.; Mena-Osteritz, E.; Bäuerle, P. *Angew. Chem., Int. Ed.* **2000**, *39*, 3481−3486.

(7) Nakao, K.; Nishimura, M.; Tamachi, T.; Kuwatani, Y.; Miyasaka, H.; Nishinaga, T.; Iyoda, M. *J. Am. Chem. Soc.* **2006**, *128*, 16740−16747.

(8) Ito, H.; Mitamura, Y.; Segawa, Y.; Itami, K. *Angew. Chem., Int. Ed.* **2015**, *54*, 159−163.

(9) Sprafke, J. K.; Kondratuk, D. V.; Wykes, M.; Thompson, A. L.; Hoffmann, M.; Drevinskas, R.; Chen, W.; Yong, C. K.; Karnbratt, J.; Bullock, J. E.; Malfois, M.; Wasielewski, M. R.; Albinsson, B.; Herz, L. M.; Zigmantas, D.; Beljonne, D.; Anderson, H. L. *J. Am. Chem. Soc.* **2011**, *133*, 17262−17273.

(10) Song, J.; Aratani, N.; Shinokubo, H.; Osuka, A. *J. Am. Chem. Soc.* **2010**, *132*, 16356−16357.

(11) Jiang, H.-W.; Tanaka, T.; Mori, H.; Park, K. H.; Kim, D.; Osuka, A. *J. Am. Chem. Soc.* **2015**, *137*, 2219−2222.

(12) Jasti, R.; Bhattacharjee, J.; Neaton, J. B.; Bertozzi, C. R. *J. Am. Chem. Soc.* **2008**, *130*, 17646−17647.

(13) Kawase, T.; Darabi, H. R.; Oda, M. *Angew. Chem., Int. Ed. Engl.* **1996**, *35*, 2664−2666.

(14) Takaba, H.; Omachi, H.; Yamamoto, Y.; Bouffard, J.; Itami, K. *Angew. Chem., Int. Ed.* **2009**, *48*, 6112−6116.

(15) Fuhrmann, G.; Debaerdemaeker, T.; Bäuerle, P. *Chem. Commun.* **2003**, 948−949.

(16) Jung, S.-H.; Pisula, W.; Rouhanipour, A.; Räder, H. J.; Jacob, J.; Müllen, K. *Angew. Chem., Int. Ed.* **2006**, *45*, 4685−4690.

(17) Kawase, T.; Seirai, Y.; Darabi, H. R.; Oda, M.; Sarakai, Y.; Tashiro, K. *Angew. Chem., Int. Ed.* **2003**, *42*, 1621−1624.

(18) Kawase, T.; Tanaka, K.; Fujiwara, N.; Darabi, H. R.; Oda, M. *Angew. Chem., Int. Ed.* **2003**, *42*, 1624−1628.

(19) Xia, J.; Bacon, J. W.; Jasti, R. *Chem. Sci.* **2012**, *3*, 3018.

(20) Iwamoto, T.; Watanabe, Y.; Sadahiro, T.; Haino, T.; Yamago, S. *Angew. Chem., Int. Ed.* **2011**, *50*, 8342−8344.

(21) Iwamoto, T.; Watanabe, Y.; Sakamoto, Y.; Suzuki, T.; Yamago, S. *J. Am. Chem. Soc.* **2011**, *133*, 8354−8361.

(22) Friend, R. H.; Gymer, R. W.; Holmes, A. B.; Burroughes, J. H.; Marks, R. N.; Taliani, C.; Bradley, D. D. C.; Dos Santos, D. A.; Bredas, J. L.; Salaneck, W. R. *Nature* **1999**, *397*, 121−128.

(23) Simeonov, A.; Matsushita, M.; Juban, E. A.; Thompson, E. H. Z.; Hoffman, T. Z.; Beuscher, A. E., IV; Taylor, M. J.; Wirsching, P.; Rettig, W.; Mccusker, J. K.; Stevens, R. C.; Millar, D. P.; Schultz, P. G.; Lerner, R. A.; Janda, K. D. *Science* **2000**, *290*, 307−314.

(24) Waldeck, D. H. *Chem. Rev.* **1991**, *91*, 415−436.

(25) Ankner, K.; Lamm, B.; Thulin, B.; Wennerstrom, O. *J. Chem. Soc., Perkin Trans. 2* **1980**, 1301−1305.

(26) Müllen, K.; Unterberg, H.; Huber, W.; Wennerstrom, O.; Norinder, U.; Tanner, D.; Thulin, B. *J. Am. Chem. Soc.* **1984**, *106*, 7514−7522.

(27) Thulin, B.; Wennerstrom, O.; Hogberg, H.-E. *Acta Chem. Scand.* **1975**, *B29*, 138−139.

(28) Thulin, B. *J. Chem. Soc., Perkin Trans. 1* **1981**, 664−667.

(29) Raston, I.; Wennerstrom, O. *Acta Chem. Scand.* **1982**, *B36*, 655−660.

(30) Zhang, F.; Götz, G.; Winkler, H. D. F.; Schalley, C. A.; Bäuerle, P. *Angew. Chem., Int. Ed.* **2009**, *48*, 6632−6635.

(31) Shabtai, E.; Segev, O.; Beust, R.; Rabinovitz, M. *J. Chem. Soc. Perkin Trans. 2* **2000**, No. 6, 1233−1241.

DOI: 10.1021/jacs.5b06258
J. Am. Chem. Soc. 2015, 137, 12282−12288

(32) Yamamoto, T.; Xu, Y.; Inoue, T.; Yamaguchi, I. *J. Polym. Sci., Part A: Polym. Chem.* **2000**, *38*, 1493−1504.
(33) Lincker, F.; Bourgun, P.; Masson, P.; Didier, P.; Guidoni, L.; Bigot, J.-Y.; Nicoud, J.-F.; Donnio, B.; Guillon, D. *Org. Lett.* **2005**, *7*, 1505−1508.
(34) Darabi, H. R.; Kawase, T.; Oda, M. *Tetrahedron Lett.* **1995**, *36*, 9525−9526.
(35) Shimizu, H.; Cojal González, J. D.; Hasegawa, M.; Nishinaga, T.; Haque, T.; Takase, M.; Otani, H.; Rabe, J. P.; Iyoda, M. *J. Am. Chem. Soc.* **2015**, *137*, 3877−3885.
(36) Carnes, M.; Buccella, D.; Decatur, J.; Steigerwald, M. L.; Nuckolls, C. *Angew. Chem., Int. Ed.* **2008**, *47*, 2982−2985.
(37) Segawa, Y.; Omachi, H.; Itami, K. *Org. Lett.* **2010**, *12*, 2262−2265.
(38) Agranat, I.; Tapuhi, Y. *J. Am. Chem. Soc.* **1976**, *98*, 615−616.
(39) Braterman, P. S.; Cross, R. J.; Young, G. B. *J. Chem. Soc., Dalton Trans.* **1977**, 1892−1897.
(40) Shekhar, S.; Hartwig, J. F. *J. Am. Chem. Soc.* **2004**, *126*, 13016−13027.
(41) Kayahara, E.; Iwamoto, T.; Suzuki, T.; Yamago, S. *Chem. Lett.* **2013**, *42*, 621−623.
(42) Segawa, Y.; Fukazawa, A.; Matsuura, S.; Omachi, H.; Yamaguchi, S.; Irle, S.; Itami, K. *Org. Biomol. Chem.* **2012**, *10*, 5979−5984.
(43) Hines, D. A.; Darzi, E. R.; Jasti, R.; Kamat, P. V. *J. Phys. Chem. A* **2014**, *118*, 1595−1600.
(44) Adamska, L.; Nayyar, I.; Chen, H.; Swan, A. K.; Oldani, N.; Fernandez-alberti, S.; Golder, M. R.; Jasti, R.; Doorn, S. K.; Tretiak, S. *Nano Lett.* **2014**, *14*, 6539−6546.
(45) Nishihara, T.; Segawa, Y.; Itami, K.; Kanemitsu, Y. *J. Phys. Chem. Lett.* **2012**, *3*, 3125−3128.
(46) Turro, N. J. *Modern Molecular Photochemistry*, 2nd ed.; University Science Books: Mill Valley, CA, 1991.
(47) Hammond, G. S.; Saltiel, J.; Lamola, A. A.; Turro, N. J.; Bradshaw, J. S.; Cowan, D. O.; Counsell, R. C.; Vogt, V.; Dalton, C. *J. Am. Chem. Soc.* **1964**, *86*, 3197−3217.

DOI: 10.1021/jacs.5b06258
J. Am. Chem. Soc. 2015, 137, 12282−12288